Published in final edited form as:
Neuron. 2009 September 10; 63(5): 614–627. doi:10.1016/j.neuron.2009.07.031.

LIG Family Receptor Tyrosine Kinase-Associated Proteins Modulate Growth Factor Signals During Neural Development

Kenji Mandai[1], **Ting Guo**[1], **Coryse St. Hillaire**[1], **James S. Meabon**[2], **Kevin C. Kanning**[2,3], **Mark Bothwell**[2], and **David D. Ginty**[1,*]

[1] The Solomon H. Snyder Department of Neuroscience, The Howard Hughes Medical Institute, The Johns Hopkins University School of Medicine, 725 North Wolfe Street, PCTB 1015, Baltimore, MD 21205, USA

[2] Department of Physiology and Biophysics, Box 357290, University of Washington, School of Medicine, Seattle, WA 98195, USA

SUMMARY

Genome-wide screens were performed to identify transmembrane proteins that mediate axonal growth, guidance and target field innervation of somatosensory neurons. One gene, *Linx* (alias *Islr2*), encoding a leucine-rich repeat and immunoglobulin (LIG) family protein, is expressed in a subset of developing sensory and motor neurons. Domain and genomic structures of Linx and other LIG family members suggest that they are evolutionarily related to Trk receptor tyrosine kinases (RTKs). Several LIGs, including Linx are expressed in subsets of somatosensory and motor neurons and select members interact with TrkA and Ret RTKs. Moreover, axonal projection defects in mice harboring a null mutation in *Linx* resemble those in mice lacking *Ngf*, *TrkA* and *Ret*. In addition, Linx modulates NGF–TrkA- and GDNF–GFRα1/Ret-mediated axonal extension in cultured sensory and motor neurons, respectively. These findings show that LIGs physically interact with RTKs and modulate their activities to control axonal extension, guidance and branching.

INTRODUCTION

During the establishment of neural circuits, neurons extend axons over long distances to innervate final target cells. In the developing peripheral nervous system (PNS), axons of sensory neurons in dorsal root ganglia (DRG) project to both a specific peripheral target, such as the skin or skeletal muscle, and one or more classes of second order neurons in the spinal cord. Similarly, spinal motor neurons project axons over long distances to their specific skeletal muscle targets in the periphery. Thus, generation of the neural circuitry underlying somatosensation and motor control relies on intricate coordination of axonal extension, guidance, branching, target recognition, synapse formation and survival of morphologically and functionally distinct subsets of sensory and motor neurons. These processes are controlled, at least in part, through the actions of secreted peptides, including neurotrophic growth factors and their receptors expressed on axons (Markus et al., 2002). However, the identity of trophic and guidance cues required for target innervation of many populations of PNS neurons and the mechanism of action of those already identified remain to be fully established.

*Correspondence: dginty@jhmi.edu.
[3]Present address: Center for Neurobiology and Behavior, Columbia University, 3701 West 168th Street, New York, NY 10032, USA

The neurotrophins are extensively characterized neurotrophic growth factors that regulate many aspects of neuronal development and function (Huang and Reichardt, 2001; Segal, 2003). The neurotrophins constitute a structurally-related family that includes nerve growth factor (NGF), neurotrophin 3 (NT3), brain-derived neurotrophic factor and neurotrophin 4. These factors activate two different classes of cell-surface receptor, the Trk receptor tyrosine kinases (RTKs) (TrkA, TrkB and TrkC) and a tumor necrosis factor receptor superfamily member, the p75 neurotrophin receptor ($p75^{NTR}$, also known as the *Ngfr* gene product) to control cell survival, differentiation and axonal growth in distinct populations of DRG sensory neurons. Another family, the glial-cell line derived neurotrophic factor (GDNF) family ligands (GFLs), also controls growth of specific subsets of both sensory and motor neurons (Airaksinen and Saarma, 2002; Baloh et al., 2000; Luo et al., 2007; Markus et al., 2002; Paratcha and Ledda, 2008). The GFL receptor complex is composed of two subunits: a glycosyl-phosphatidylinositol-anchored ligand binding coreceptor, GDNF family receptor α (Gfrα1–4), and a signaling subunit, the Ret RTK.

Trk and Ret RTKs are expressed in distinct populations of embryonic DRG sensory and spinal motor neurons where they control axonal development, target innervation and neuronal survival (Baloh et al., 2000; Bennett et al., 1998; Huang and Reichardt, 2001; Luo et al., 2007; Mu et al., 1993). TrkA, TrkB and TrkC are mainly found in small diameter nociceptive neurons, subsets of medium-to-large diameter mechanosensory neurons, and large diameter mechanosensory and proprioceptive neurons, respectively. TrkB is also found in a subset of spinal motor neurons. Ret, in contrast, is expressed in small diameter, non-peptidergic DRG sensory neurons, a subset of large diameter sensory neurons, and virtually all spinal motor neurons. Using mouse model systems, it is observed that differential patterns of expression of neurotrophins, GFLs and their receptors enables sensory and motor neurons to innervate distinct targets (Airaksinen et al., 1996; Baloh et al., 2000; Crowley et al., 1994; Ernfors et al., 1994; Gould et al., 2008; Huang and Reichardt, 2001; Luo et al., 2007; Smeyne et al., 1994; Tessarollo et al., 1994). There are several examples of this, including: (1) NGF–TrkA signaling mediates extension and branching of peripheral axonal projections of small caliber nociceptors (Patel et al., 2000; Wickramasinghe et al., 2008); (2) NT3–TrkC signaling controls both peripheral and central axonal projections of large diameter proprioceptive neurons (Patel et al., 2003); and (3) GDNF–GFRα1/Ret, in cooperation with EphA4, guides axons of a subset of lateral motor column (LMC)(l) motor neurons to the dorsal muscles of the hindlimb (Kramer et al., 2006a).

Although neurotrophic factor receptors are expressed in select subsets of neurons, they alone cannot account for the specificity or uniqueness of the patterns of PNS axonal projections to central and peripheral target fields. For instance, TrkC is expressed in most, if not all large diameter DRG sensory neurons that innervate muscle spindles, Golgi tendon organs, and Merkel cells in the skin, and NT3–TrkC signaling is required for target innervation of these neuronal populations (Airaksinen et al., 1996; Ernfors et al., 1994; Patel et al., 2003). Therefore, it would appear that, in addition to NT3, additional cues must be present for axonal targeting of these functionally and morphologically distinct classes of large-diameter $TrkC^{+}$ sensory neurons. Likewise, Ret is expressed in virtually all spinal motor neurons (Garces et al., 2000; Gould et al., 2008), and yet GDNF–GFRα1/Ret signaling appears only required for targeting of a subset of LMC(l) motor neurons to the dorsal hindlimb (Kramer et al., 2006a). Here again, additional cues other than GDNF are likely to support growth of Ret-expressing LMC neurons into their target fields. Indeed, considerable evidence implicates members of the semaphorin, ephrin and netrin families of guidance cues in the control of PNS axonal projections (Tran et al., 2007). Another plausible mechanism to achieve specificity of circuit formation is cell-type specific modulation of axonal growth and guidance responses to individual cues. Whether Trk- and Ret-signals are modulated to confer cell type-specific responses to their respective ligands during development of sensory and motor circuits remains to be determined.

To obtain a better understanding of the specificity of axonal growth, guidance and target field innervation of unique populations of somatosensory neurons, we performed genome-wide screens to identify transmembrane proteins expressed in distinct neuronal subsets. Our goal was to identify novel receptor components or modulators of known receptor systems that control the development of PNS circuits. Here, we report the identification and characterization of Linx, a leucine-rich repeat and immunoglobulin (LIG) family transmembrane protein that is structurally related to Trk receptors. Linx is expressed in a subset of DRG sensory and spinal motor neurons and physically interacts with both Trk and Ret RTKs. Moreover, defects in sensory and motor axonal projections in *Linx* mutant mice resemble those found in mice lacking *Ngf* and *TrkA*, and *Ret*, respectively. In addition, Linx is one of 18 members of a newly identified LIG gene family (MacLaren et al., 2004), several of which we find to be expressed in subsets of developing sensory and motor neurons and interact with Trk and Ret RTKs. Taken together, our findings support a model in which LIG family members form complexes with RTKs in unique populations of developing neurons and modulate their activities to control specific stages of sensory and motor neuron axon growth, guidance and branching.

Results

Linx, a LIG Family Member Expressed in a Subset of DRG Neurons

To identify proteins that control axonal projections of DRG sensory neurons, we searched for genes encoding transmembrane proteins expressed in unique populations of developing DRG neurons. We reasoned that such transmembrane proteins are candidates to mediate axonal growth and guidance decisions of different neuronal classes as they project to their unique targets in the spinal cord and periphery. Thus, genome-wide gene profiling analysis was performed using DNA microarrays for RNA prepared from DRGs obtained from wild-type and mutant embryos lacking specific populations of embryonic DRG neurons. To ablate specific populations of neurons in the DRG, we exploited the respective trophic factor dependencies of these populations. E14.5 mouse DRGs were collected, and comparisons were performed between $Ngf^{-/-}$ and wild-type controls, and between $Ntf3^{-/-}$ (alias *NT3*) mice and wild-type controls. At E14.5, most small diameter, $TrkA^+$ neurons are eliminated in $Ngf^{-/-}$ DRG (Crowley et al., 1994) (data not shown). Conversely, many $TrkA^+$ neurons survive in $Ntf3^{-/-}$ mice, whereas virtually all large diameter $TrkC^+$ neurons are lost (Ernfors et al., 1994; Tessarollo et al., 1994) (data not shown). Therefore, genes preferentially expressed in $TrkA^+$ DRG neurons should display lower levels of expression in $Ngf^{-/-}$ DRG than wild-type DRG and, conversely, relatively higher levels of expression in $Ntf3^{-/-}$ DRG than wild-type DRG. Our analyses identified more than 110 genes that exhibited lower levels of expression in $Ngf^{-/-}$ DRG compared to wild-type DRG, including those known to be expressed in small diameter neurons such as *Ntrk1/TrkA* itself, *Runx1* and *Scn10a/$Na_V1.8$* (Akopian et al., 1996; Chen et al., 2006; Kramer et al., 2006b; Marmigere et al., 2006) (Table S1). Conversely, 10 genes exhibited lower expression in $Ntf3^{-/-}$ DRG compared to wild-type DRG, including *Etv1/ER81*, which is expressed in large diameter neurons (Lin et al., 1998) (Table S2).

Our screen also identified many uncharacterized genes, including the genes that we sought, encoding putative transmembrane proteins. Among those preferentially expressed in $TrkA^+$ DRG neurons, one gene encodes a transmembrane protein with 5-tandemly linked leucine-rich repeat (LRR) domains, flanked by LRR N-terminal and C-terminal cysteine-rich domains (LRRNT and LRRCT, respectively), an immunoglobulin (IG) domain, a transmembrane domain and a short cytoplasmic tail. The amount of transcripts of this gene is lower in $Ngf^{-/-}$ DRG compared to wild-type DRG, and higher in $Ntf3^{-/-}$ DRG compared to wild-type DRG (Tables S1 and data not shown). We named this gene product Linx (leucine-rich repeat domain and immunoglobulin domain containing axon extension protein, also known as the *Islr2* gene product) (Figure 1A). Linx has a high degree of homology with Islr, a protein whose

function is unknown. Islr lacks a transmembrane and intracellular domain (Nagasawa et al., 1997). Linx and Islr exhibit nearly 61% amino acid identity in the regions containing their LRRNT, LRR and LRRCT domains. As predicted, cell surface biotinylation experiments showed that Linx is localized to the cell surface (Figure S2A).

Both Linx and Islr are members of the LIG family of proteins (MacLaren et al., 2004). The extent of sequence similarity of the extracellular domains among the 18 human LIG proteins is displayed as a tree dendrogram in Figure 1B. These sequence homologies suggest that LIG proteins including those encoding the three Trk receptors are evolutionarily related and, therefore, the Trk genes may have evolved from a gene whose translational product is an ancestral LIG protein lacking a tyrosine kinase domain. A striking feature of the *LIG* genes, both in humans and Drosophila, is that they are not uniformly distributed throughout the genome but rather they are clustered (Figure S1 and Table S3). Statistical analysis of the clustering of the human *LIG* genes, using a Monte Carlo method, indicates that this degree of clustering is unlikely to have occurred by chance (p=0.008). Additional support for the idea that *LIGs* have arisen from a common ancestral gene comes from the similarities of the exon structure of these genes. Except the *LRIG* and *TRK* paralogs, many of the human *LIG* genes have the unusual feature of having their open reading frame contained within a single exon, or in a few cases, a short exon encoding the leader sequence and the remainder encoded by a single exon (Table S3).

LIG Family Proteins Interact with TrkA, Ret and p75^{NTR}

Previous studies demonstrated that the LIG family member Lrig1 binds to the ErbB, Met and Ret RTKs (Gur et al., 2004; Laederich et al., 2004; Ledda et al., 2008; Shattuck et al., 2007). In addition, Lingo-1 and Lrig3 bind ErbB1 as well as p75^{NTR} and FGF receptor 1, respectively (Inoue et al., 2007; Mi et al., 2004; Zhao et al., 2008). Thus, we hypothesized that other LIG proteins, including Linx may also interact with RTKs. Therefore, physical interactions between LIG proteins and TrkA, TrkB, TrkC and Ret, major RTKs expressed in DRG neurons, as well as EphA4 were assessed. Co-immunoprecipitation experiments using 293T cells demonstrated that each of the 5 LIG proteins tested, including Linx, but not FGFR2, a negative control, was efficiently co-immunoprecipitated with TrkA (Figure 2A). To further characterize the interaction between TrkA and Linx, we performed immunoprecipitation experiments using cultured E13.5 DRG sensory neurons. Our findings indicate that endogenous Linx forms a stable complex with TrkA in sensory neurons (Figure 2B). Moreover, acute application of NGF does not affect the extent of the interaction between Linx and TrkA (data not shown). We also determined the extent of colocalization of endogenous Linx and TrkA using cultured E13.5 DRG sensory neurons. Indeed, endogenous TrkA and Linx were colocalized to punctae along axons of these neurons, although some punctae contained only TrkA or Linx (Figure 2C). Furthermore, domain structure-function analysis using the 293T cell immunoprecipitation assay indicates that the interaction between Linx and TrkA is mediated through their extracellular domains (Figures S2C and S2D) and that Linx can form homo-multimers (Figure S2E). Moreover, each of the LIG proteins examined can interact with TrkC whereas little to no interaction is detected between LIGs and TrkB (Figures 2D and 2E). Interactions between LIGs and RTKs were not limited to the Trk receptors as several LIG family members were found to interact with Ret and p75^{NTR} (Figures 2F and S2F). Finally, LIGs do not associate with EphA4 (Figure S2G), another RTK, which controls motor axon growth into the periphery (Helmbacher et al., 2000). Together, these observations suggest that LIG family members may regulate or modulate TrkA, TrkC, Ret and p75^{NTR} signaling in the developing PNS neurons.

Generation of *Linx* Null Mice

To assess the *in vivo* function of Linx and its interactions with the abovementioned RTKs during development of PNS projections, and to visualize axons of Linx^{+} neurons, we generated

a *Linx* mutant mouse in which a *Tau-EGFP (enhanced green fluorescent protein)* reporter gene was inserted into the exon coding the entire coding sequence of *Linx* (Figure S3A). This null allele containing an EGFP-tagged disruption of *Linx* is referred to as $Linx^{+/tEGFP}$. Southern blot analysis confirmed homologous recombination, germline transmission and removal of a *TK-Neo* cassette after crossing with mice expressing Cre recombinase in the germ cell lineage (Figure S3B).

Linx Expression in the Spinal Cord and Peripheral Nervous System

To further characterize Linx expression in the PNS, we generated a Linx antibody. Immunoblot analysis using the Linx antibody and brain lysates from $Linx^{tEGFP/tEGFP}$ mice confirmed both the specificity of the antibody and that the *Tau-EGFP* reporter insertion indeed abolished Linx expression in $Linx^{tEGFP/tEGFP}$ mice (Figure S3C). Also, immunohistochemical analysis using the Linx antibody and brain sections from $Linx^{tEGFP/tEGFP}$ mice detected very little immunoreactive signal confirming the high specificity of this reagent (data not shown).

At E11.5, Linx protein is robustly detected in spinal nerves, their roots and the ventral spinal cord whereas it is not detected in the soma of the DRG neurons themselves (Figure 3A). These data are consistent with previous findings using *in situ* hybridization (Gejima et al., 2006) and suggest that Linx is expressed in motor neurons but not in sensory neurons at this time point. The expression of Linx in the nervous system appears highly specific as little to no staining was observed in peripheral tissues. At a later time, E12.5, Linx protein is detected in the ventral spinal cord, DRG, dorsal and ventral roots and sympathetic chain ganglia (Figures 3B). Anti-GFP immunostaining of sections from $Linx^{+/tEGFP}$ mice revealed that *Linx* is expressed in nearly all Ret^{+} motor neurons at E12.5 (Figure 3C) and in essentially all $TrkA^{+}$ DRG sensory neurons at E14.5 (Figure 3E). *Linx* is not expressed in $TrkB^{+}$, $TrkC^{+}$ or $p75^{NTR+}$ DRG sensory neurons at E14.5 or E17.5 (Figures S4A to S4C). In contrast, at E18, only a subset of $TrkA^{+}$ DRG sensory neurons expresses *Linx* (Figures 3F), while nearly all Ret^{+} motor neurons express *Linx* (Figures 3D). The population of DRG sensory neurons expressing Linx gradually decreases from E14.5 to P7 (Figures 3E, 3F and S4D). Whole-mount immunostaining using the Linx antibody reveals that Linx is localized on spinal nerves and their branches in the extremities (Figure 3G and data not shown). Thus, *Linx* is expressed in motor, sensory and sympathetic neurons, and Linx protein is enriched on the axons of these neurons where it colocalizes and physically interacts with RTKs that control development of their axonal projections.

Linx Mutant Mice Partially Phenocopy *Ret, Ngf* and *TrkA* Mutant Mice

To establish the function of Linx during development of DRG sensory and spinal motor neuron axonal projections, whole-mount anti-Peripherin immunostaining was performed to visualize these axons in embryos. Because Linx is associated with axon bundles of spinal nerves and their roots (Figures 3A, 3B and 3G), we mainly focused our analysis on spinal nerve projections in the hindlimbs. At E12.5, striking defects were observed in hindlimb nerves in $Linx^{tEGFP/tEGFP}$ embryos. Both the common peroneal and tibial nerves, which originate from the sciatic nerve and project to the distal hindlimb, were shorter and thinner, especially in the distal limb (Figures 4A and 4B). At E13.5, the common peroneal nerve in $Linx^{tEGFP/tEGFP}$ embryos was much thinner than in wild-type controls (Figures 4C–4E). Moreover, in $Linx^{tEGFP/tEGFP}$ embryos, the superficial and deep branches of the common peroneal nerve were stalled (Figures 4C, 4D and 4F) and, remarkably, the sural and saphenous nerves apparently compensated for this deficit by supplying branches to the regions normally innervated by peroneal nerve branches (Figure 4D). To visualize motor neuron projections in $Linx^{tEGFP/tEGFP}$ embryos, the *Linx* mutants were crossed with an *Hb9-Gfp* transgenic reporter line (Wichterle et al., 2002) (Figures S5A–S5F). Whole-mount immunostaining analyses using $Linx^{tEGFP/tEGFP}$*;Hb9-Gfp* compound mutants clearly showed that axons of motor neurons in

the peroneal nerves of *Linx*$^{tEGFP/tEGFP}$ embryos are more prominently stalled than those of sensory neurons. This peroneal nerve defect persists in *Linx*$^{tEGFP/tEGFP}$ mice until at least by P0 (Figures S8G and S8H), the latest time of analysis since these mice die. Interestingly, the peroneal nerve defects were not found in *Ngf*$^{-/-}$ embryos (Figure S6). The tibial nerve was also underdeveloped in *Linx*$^{tEGFP/tEGFP}$ embryo (Figures S7A–S7C). As motor neuron cell death caused by a lack of final target innervation may confound analysis of axon targeting, we used a *Bax*$^{-/-}$ genetic background in which spinal motor neuron apoptosis is absent (White et al., 1998) to circumvent this issue. *Linx*$^{tEGFP/tEGFP}$*;Bax*$^{-/-}$ compound mutant mice exhibited a similar peroneal nerve phenotype in *Linx*$^{tEGFP/tEGFP}$ mice (Figures S8A–S8C), indicating that neuronal cell death (Figure S8D) is not the cause of the peroneal nerve defect in mice lacking *Linx*.

Interestingly, the dramatic peroneal nerve defect in *Linx*$^{tEGFP/tEGFP}$ embryos is reminiscent of that reported for *Ret*$^{-/-}$ embryos (Gould et al., 2008; Kramer et al., 2006a). Therefore, we directly compared *Ret*$^{-/-}$ embryos to *Linx*$^{tEGFP/tEGFP}$ embryos at both E12.5 and E13.5. As reported (Kramer et al., 2006a), at E12.5, the extension of the common peroneal nerve in *Ret*$^{-/-}$ embryos was grossly underdeveloped, compared to control embryos, especially in the distal limb (Figures 4G and 4H). At E13.5, the common peroneal nerve in *Ret*$^{-/-}$ embryos is much thinner than in control embryos (Figures 4I, 4J and 4E) although, as reported (Gould et al., 2008; Kramer et al., 2006a), large variations in the expressivity of this phenotype were observed. In spite of the variability, the average diameter of the *Ret*$^{-/-}$ common peroneal nerve was similar to that of *Linx*$^{tEGFP/tEGFP}$ embryos. Also similar to the *Linx*$^{tEGFP/tEGFP}$ embryos, extension of the superficial and deep branches of the common peroneal nerve was markedly stunted in *Ret*$^{-/-}$ embryos (Figures 4I, 4J and 4F). However, the *Linx*$^{tEGFP/tEGFP}$ embryos do not completely phenocopy *Ret*$^{-/-}$ embryos because, unlike *Linx*$^{tEGFP/tEGFP}$ embryos, the tibial nerve in *Ret*$^{-/-}$ embryos was similar to that of wild-type embryos (Figure S7D). To test the possibility of a genetic interaction between *Linx* and *Ret*, we generated *Linx;Ret* compound mutant mice and measured the length of the deep peroneal nerve of mice lacking one or both alleles of both *Ret* and *Linx* at E13.5. As above, *Linx*$^{tEGFP/tEGFP}$ embryos displayed shorter deep peroneal nerves than control littermates (Figure 5C). Interestingly, this phenotype was enhanced by removing a single copy of *Ret* (Figure 5D), although the *Ret* heterozygote itself did not exhibit a phenotype (Figures 5A and 5B). Furthermore, the nerve was significantly shorter in *Linx*$^{tEGFP/tEGFP}$*;Ret*$^{-/-}$ embryos than the *Linx*$^{tEGFP/tEGFP}$ embryos (Figure 5E). Thus, we conclude that *Linx*$^{tEGFP/tEGFP}$ mice partially phenocopy *Ret*$^{-/-}$ mice and that there are both *Linx*-dependent and *Linx*-independent *Ret* signaling pathways controlling development of the deep peroneal nerve (Figure 5F).

The observations that *Linx*$^{tEGFP/tEGFP}$ embryos partially phenocopy *Ret*$^{-/-}$ embryos, that *Ret* and *Linx* may interact genetically, and that Linx and Ret form a physical complex suggest that GDNF–GFRα1/Ret signaling is dependent on Linx. To address this possibility, we cultured lumbar motor neurons obtained from E13.5 *Linx*$^{tEGFP/tEGFP}$ and *Linx*$^{+/tEGFP}$ control embryos in growth media containing CNTF (10 ng/ml), which prevents cell death, and either the presence or absence of GDNF (10 ng/ml) for 24h. Motor neurons were then identified by immunocytochemistry using GFP and Islet1 antibodies, and the longest axons of each neuron were measured. Under these conditions, GDNF-dependent axonal extension was observed in control cultures (Figure 5G). Remarkably, motor neurons from *Linx*$^{tEGFP/tEGFP}$ embryos showed reduced or absent GDNF-dependent axonal extension compared to *Linx*$^{+/tEGFP}$ control motor neurons. These observations indicate that Linx is required in a subset of spinal motor neuron axons as they project into the dorsal region of the distal hindlimb, probably through the direct physical interaction with the Ret RTK and modulation of GDNF–GFRα1/Ret signaling.

In addition to its role in Ret signaling, Linx is a candidate to modulate NGF–TrkA signaling in developing sensory neurons because it is expressed in $TrkA^+$ DRG sensory neurons, can form a physical complex with endogenous TrkA, and at least partially colocalizes with TrkA in sensory neuron axons. Therefore, we next assessed whether Linx is required for extension or branching of $TrkA^+$ somatosensory neurons in the distal hindlimbs. Here, the extension of the digital branch of the deep peroneal nerve into the 3rd digit was examined at E14.5. This branch is mainly composed of sensory fibers (Figures S5C, S5I and S5J). The length of this nerve was reduced by nearly 18% in $Linx^{tEGFP/tEGFP}$ embryos compared to wild-type controls (Figures 6A–6D and 6I). Next, 6we measured the length of the lateral branch of the lateral plantar nerve in the 5th digit, a branch of the tibial nerve, that is also mainly composed of sensory fibers and innervates lateral plantar skin (Figures S5K and S5L) (Povlsen et al., 1994). This projection was found to be reduced by nearly 9% in $Linx^{tEGFP/tEGFP}$ embryos compared to wild-type controls at E14.5 (Figures 6E–6H and 6J). NGF is required for the establishment of cutaneous sensory innervation (Patel et al., 2000; Wickramasinghe et al., 2008) and, therefore, we asked whether $Ngf^{-/-}$ and $TrkA^{-/-}$ embryos exhibit similar defects in the branches of the common peroneal nerve and lateral plantar nerve. To address this question, we used mice harboring compound mutations in *Ngf* or *TrkA*, and *Bax* to circumvent the confounding issue of cell death for the analysis. DRG neurons that normally die in the absence of either NGF or TrkA survive in a $Bax^{-/-}$ background (Patel et al., 2000). Indeed, both $Ngf^{-/-};Bax^{-/-}$ and $TrkA^{-/-};Bax^{-/-}$ embryos displayed deficits of nerve extension in the hindlimbs at E14.5, similar to that seen in the $Linx^{tEGFP/tEGFP}$ mouse. The extension of the 3rd digital branch of deep peroneal nerve was reduced by nearly 27% in $Ngf^{-/-};Bax^{-/-}$ embryos compared to littermate control embryos (Figures 6K–6N and 6S), and the extension of the branch of the lateral plantar nerve was reduced by nearly 13% and 9% in $Ngf^{-/-};Bax^{-/-}$ and $TrkA^{-/-};Bax^{-/-}$ embryos, respectively, compared to individual controls (Figures 6O–6R, 6T and S9A–S9G). The similarity of phenotypes observed in the lateral plantar nerves in $Linx^{tEGFP/tEGFP}$, $Ngf^{-/-};Bax^{-/-}$ and $TrkA^{-/-};Bax^{-/-}$embryos at E14.5 indicates that *Linx* mutant mice partially phenocopy *Ngf* and *TrkA* mutants. This is consistent with the idea that Linx modulates NGF–TrkA signals that control axonal extension.

In addition to axonal extension, NGF regulates axonal branching (Lentz et al., 1999). Indeed, sensory neuron axonal branching in the distal extremities is impaired in $Ngf^{-/-};Bax^{-/-}$ embryos (Wickramasinghe et al., 2008). Therefore, we next asked whether $Linx^{tEGFP/tEGFP}$ embryos exhibit deficits in branching of sensory axons within peripheral nerves. Both the number of branches and the orders of branches in the medial digital branch of lateral plantar nerve in the 5th digit of $Linx^{tEGFP/tEGFP}$ embryo were markedly impaired compared to control embryos at E15.5 (Figures 7A–7F). As may be expected, a nearly identical phenotype was observed in both $Ngf^{-/-};Bax^{-/-}$ (Figures 7G–7K) and $TrkA^{-/-};Bax^{-/-}$ embryos (Figures S9H–S9O). These results suggest that *Linx*, *Ngf* and *TrkA* regulate the extension and branching of sensory fibers predominantly in the distal regions of their projections. The number of neuronal cell bodies in L5 DRG at E13.5 in $Linx^{tEGFP/tEGFP}$ embryos was not different from wild-type embryos (Figure S8E), although 16% fewer neurons are observed at E15.5 in $Linx^{tEGFP/tEGFP}$ embryos (Figure S8F). Therefore, there are cell survival defects at E15.5, and axonal extension and branching defects at E14.5 and E15.5, respectively, in $Linx^{tEGFP/tEGFP}$ embryos. Thus, at least some of the axonal growth and branching deficits found in $Linx^{tEGFP/tEGFP}$ embryos are similar to those found in $Ngf^{-/-}$ and $TrkA^{-/-}$ embryos, suggesting that Linx serves as a modulator of NGF–TrkA signaling.

To further assess the functional interaction between Linx and NGF–TrkA signaling, we asked whether Linx modulates NGF-dependent neurite outgrowth of cultured DRG sensory neurons. Here, DRG neurons from $Linx^{tEGFP/tEGFP}$ and $Linx^{+/tEGFP}$ control embryos taken from E13.5 mice were cultured for 24 hr in media containing either 0, 3, 9, or 27 ng/ml NGF and Boc-aspartyl (OMe)-fluoromethylketone (BAF), which prevents apoptotic cell death. Then, the

longest axonal projections of each neuron were measured, after double immunostaining using GFP and Neurofilament-M antibodies (Figure 7L). *Linx*$^{tEGFP/tEGFP}$ sensory neurons exhibit reduced axonal extension when grown in media containing 3 and 9 ng/ml NGF compared to control *Linx*$^{+/tEGFP}$ DRG sensory neurons. Finally, we examined the phosphorylation status of TrkA as well as its effectors Akt and Erk, which control axonal extension in sensory neurons (Huang and Reichardt, 2001; Segal, 2003), following stimulation of cultured DRG neurons obtained from E13.5 *Linx*$^{tEGFP/tEGFP}$ and wild-type control embryos with 10 ng/ml NGF. In *Linx*$^{tEGFP/tEGFP}$ DRG neurons, NGF-dependent phosphorylation of Erk was consistently decreased (Figure 7N), although the expression of TrkA and its autophosphorylation at Y490 and the phosphorylation of Akt following NGF stimulation were comparable in *Linx*$^{tEGFP/tEGFP}$ and wild-type embryos (Figures 7M and 7O). These observations indicate that Linx is dispensable for NGF stimulation of TrkA autophosphorylation, but modulates axonal extension and is required for maximum NGF–TrkA signaling in sensory neurons.

Somatosensory and Motor Neuron Expression of *LIG* Family Members

Our findings indicate that Linx modulates RTK signaling in developing spinal motor and DRG sensory neurons through direct physical interactions with Ret and TrkA, respectively. Moreover, cell culture experiments have indicated that other *LIG* family members may diminish RTK signaling events in other cell types (Inoue et al., 2007; Laederich et al., 2004; Ledda et al., 2008). To determine whether additional *LIG* family members are expressed in DRG sensory and spinal motor neurons, double-label *in situ* hybridization was performed for five representative members of the major subfamilies of *LIG* genes, as well as *TrkA* or *Ret*, using E13.5 wild-type lumbar spinal cord and DRG sections. Strikingly, most of these *LIGs* are expressed in distinct subsets of DRG sensory neurons (Figure 8A). Among the five *LIGs* examined, *Linx* is expressed in nearly all *TrkA*$^{+}$ neurons, whereas *Lingo1* is expressed in a subset of medium and large diameter *TrkA*$^{-}$ neurons. *Lrrc4b* is expressed in a subset of small diameter *TrkA*$^{+}$ neurons and a subset of medium and large diameter *TrkA*$^{-}$ neurons. *Amigo1* is expressed in nearly all *TrkA*$^{+}$ neurons as well as a subset of medium and large diameter *TrkA*$^{-}$ neurons. *Lrig1* is undetectable in E13.5 DRG (data not shown). In addition, expression of several LIGs was detected in cultured DRG neurons by quantitative reverse transcriptase-polymerase chain reaction (qRT-PCR) using RNA purified from E13.5 DRG explant cultures, and exposure of neurons to NGF enhanced expression of both *TrkA* and *Linx*, while it did not change expression of other *LIG* genes examined (Figure 8B). Moreover, our *in situ* hybridization analysis revealed that *Linx*, *Lingo1* and *Lrrc4b* are expressed in motor neurons in the lumbar spinal cord, while *Amigo1* and *Lrig1* are not (Figure 8C and data not shown). Together, these observations indicate that, like Linx, several LIG family members may control development of select populations of motor and sensory neurons by modulating the functions of Ret, Trks, or other RTKs during distinct stages of axonal extension, guidance, branching and target innervation.

Discussion

Here, we report identification and characterization of Linx, a LIG family transmembrane protein that is structurally related to Trk RTKs. It is expressed in a subset of DRG sensory and spinal motor neurons and physically interacts with RTKs, including TrkA and Ret. Moreover, *Linx* mutant mice exhibit sensory and motor neuron axonal projection defects similar to but milder than those found in *Ngf*, *TrkA* and *Ret* mutant mice. Furthermore, NGF- and GDNF-dependent axonal outgrowth is impaired in cultured sensory and motor neurons, respectively, lacking Linx. Finally, several other LIG family members are expressed in subsets of DRG sensory and spinal motor neurons, and interact with Trk and Ret RTKs. These observations support a model in which LIG family members form complexes with RTKs in distinct

populations of developing sensory and motor neurons to modulate their activities to control specific stages of axonal growth, branching and circuit formation.

Linx: a modulator of NGF–TrkA and GDNF–Ret Signaling

This present work reveals a role for Linx in both NGF–TrkA and GDNF–Ret signaling during development of PNS projections. We find that Linx modulates GDNF–Ret signaling, at least during development of the deep peroneal nerve, and NGF–TrkA signaling during axonal growth of cutaneous sensory neurons. However, *Linx*$^{tEGFP/tEGFP}$ embryos do not completely phenocopy embryos lacking NGF or TrkA since much less neuronal death was observed in DRGs of *Linx* mutants, compared to *Ngf*$^{-/-}$ and *TrkA*$^{-/-}$embryos (Figure S8). Therefore, Linx appears to be a modulator of both NGF–TrkA and GDNF–Ret signals that control axonal growth; Linx has relatively little impact on the control of neuronal survival.

The analysis of *Linx*$^{tEGFP/tEGFP}$*;Hb9-Gfp* mice indicates that the peroneal nerve defect observed in *Linx*$^{tEGFP/tEGFP}$ mice is primarily due to impaired development of motor axons (Figures S5A–S5F). Evidence to support the notion that *Linx* is required cell autonomously in motor neuron is that Linx is expressed in motor neurons but not in DRG sensory neurons at E11.5 and in a subset of DRG sensory neurons at E12.5 (Figures 3A–3C), when the peroneal nerve is already dramatically defective (Figures 4A and 4B). Furthermore, *Ret* is required in motor neurons for development of the peroneal nerve (Gould et al., 2008; Kramer et al., 2006a), the *Linx* mutant mouse partially phenocopies the *Ret* mutant (Figure 4) and *Linx* and *Ret* appear to genetically interact (Figure 5). We therefore speculate that any sensory projection deficit associated with the deep peroneal nerve results from a lack of interaction between motor and sensory axons (Gallarda et al., 2008). In contrast, defects in the lateral plantar nerve branches of *Linx* mutants are almost certainly the result of primary defects in sensory nerves because these branches are mainly composed of sensory fibers (Figures S5K and S5L) (Povlsen et al., 1994), and similar defects are found in *Ngf*$^{-/-}$*;Bax*$^{-/-}$ and *TrkA*$^{-/-}$*;Bax*$^{-/-}$ mice, which do not exhibit motor neuron defects. It will be of interest to determine whether and how Linx modulates: 1) binding of ligands to RTK complexes; 2) cell surface localization of RTKs; 3) endocytosis of ligand-bound RTKs; and 4) signaling and retrograde transport of signaling endosomes containing ligand-bound receptor complexes. The observations that NGF activates TrkA autophosporylation on Y490, the Shc binding site, and phosphorylation/activation of Akt in neurons from *Linx*$^{tEGFP/tEGFP}$ mice suggest that ligand-dependent activation of cell surface TrkA and at least some TrkA effectors occurs normally in the absence of *Linx* (Figures 7M and 7O).

It will also be interesting to determine how binding specificity between LIG family members and RTKs is achieved. Indeed, the mechanism by which Linx associates with TrkA and TrkC but not the close family member, TrkB is unclear. Our findings do indicate that the extracellular domain of TrkA, but not TrkB, is sufficient to mediate its interaction with Linx (Figure S2D). Further structure-function analysis of the domains involved in Linx-Trk interactions and identification of the subcellular locale of these interactions should shed light on this issue. It will also be of interest to determine the functional significance of the interaction between Linx and TrkC or p75^{NTR} in neurons other than DRG sensory neurons.

LIGs: Modulators of Receptor Tyrosine Kinase Signaling

Our analysis of the structures of *LIG* genes suggests that the 18 human *LIG* genes, including the three *TRK* genes, evolved from a common ancestral *LIG* gene. Since *LIG* genes exist in sea urchins and vertebrates (Deuterostomes) as well as insects (Protostomes), *LIG* genes apparently had already evolved from a common ancestor of Protostomes and Deuterostomes. The existence of 6 subfamilies of *LIG* genes each containing 2 to 4 members, as well as the distribution of members of subfamilies on various human chromosomes is consistent with the

idea that the ancestral *LIG* gene underwent several tandem gene duplication events, leading to genetically linked *proto-TRK*, *proto-LINGO*, *proto-AMIGO*, *proto-LRIG*, *proto-LINX* and *proto-LRRC4* genes. Following genome duplication events, early vertebrate evolution generated paralogous copies of this gene cluster.

With the exception of Trks, which are well-characterized neurotrophin receptors, the *in vivo* functions of most mammalian LIG proteins are not well understood. Remarkably, Lingo-1 may function as a coreceptor for the $p75^{NTR}$/NgR1 and Troy/NgR1 receptor complexes to inhibit neurite outgrowth and regulate myelination by oligodendrocytes and neuronal cell survival (Fu et al., 2008; Inoue et al., 2007; Mi et al., 2004). It is interesting to note that our findings show that Linx can also form a complex with $p75^{NTR}$. Lingo-1 also directly binds to ErbB1 and negatively regulates its function (Fu et al., 2008; Inoue et al., 2007). The NGL subfamily, containing NGL-1/Lrrc4c and NGL-2/Lrrc4, are implicated as binding partners of Netrins G1 and G2, possibly representing a novel cell adhesion system controlling outgrowth of thalamocortical axons and regulators of excitatory synapse formation (Kim et al., 2006; Lin et al., 2003). The Amigo subfamily containing Amigo1, Amigo2/Alivin 1 and Amigo3 is implicated in cell adhesion events that control axon extension and fasciculation of axon bundles (Kuja-Panula et al., 2003). Amigo2/Alivin 1 also controls survival of cerebellar granule neurons (Ono et al., 2003). While our characterization of Linx suggests that it augments neurotrophin and GFL signaling through physical interactions with Trk and Ret receptors, respectively, some Lrig subfamily members are known to inhibit RTK signaling events. Lrig1 can directly interact with ErbB and Met and function to attenuate RTK signaling by enhancing degradation of these receptors (Gur et al., 2004; Inoue et al., 2007; Laederich et al., 2004; Shattuck et al., 2007). Similarly, Lrig3 can directly interact with FGF receptor 1, decrease its expression and attenuate FGF signaling in animal caps of *Xenopus* (Zhao et al., 2008). Interestingly, our immunoprecipitation experiments also revealed decreased expression of certain RTKs as well as $p75^{NTR}$ when either Lingo1 or Lrig1 were expressed simultaneously with these receptors (Figures 2A, 2D–2F, S2B, S2F and S2G). Further studies will be required to determine whether Lingo1 and Lrig1 facilitate receptor degradation through a common mechanism. Lrig1 also directly interacts with Ret and negatively regulates GDNF–Ret signaling through inhibition of GDNF binding to the Ret complex and recruitment of Ret to lipid rafts (Ledda et al., 2008). Thus Linx, Lrig subfamily members and Lingo-1 physically interact with RTKs and modulate their functions in an opposing manner in cells that coexpress these LIGs. Together with the findings that Linx and other LIG family members are expressed in subsets of neurons and that expression of LIGs varies with age, we suggest that these proteins differentially augment or attenuate RTK signaling events in spatially and temporally controlled manners to provide fine modulation of growth factor signaling events during axonal growth and guidance.

The functions of LIG family members are likely to extend beyond axonal growth, guidance and branching and include roles in both development and maintenance in the adult, perhaps even contributing to certain pathologies. Indeed, *LRIG1* and *LRRC4* have been implicated as tumor suppressor genes for several human cancers (Hedman and Henriksson, 2007; Wu et al., 2006). The full spectrum of *in vivo* functions of Linx and other LIG family members during development and in the adult awaits comprehensive analyses of mutant mice lacking each member of the *LIG* family and identification of their RTK binding partners. We propose that LIGs have evolved to both positively and negatively modulate RTK signaling events to provide fine-tuned control over growth factor signaling pathways. In this way, LIGs increase the repertoire of growth factor signaling intensities and events, regulated by a limited number of growth factors and their receptors to control the complexities of neural connectivity and other functions during development and in adult organisms.

EXPERIMENTAL PROCEDURES

Mouse Lines

The mouse lines used in this study were maintained on a C57BL/6 background. These are: *Ngf*$^{+/-}$ (Crowley et al., 1994), *Bax*$^{+/-}$ (Knudson et al., 1995), *TrkA*$^{+/-}$ (Moqrich et al., 2004), *Ntf3*$^{+/-}$ (Tessarollo et al., 1994) and *Hb9-Gfp* (Wichterle et al., 2002). *FLAG epitope tagged-TrkA* knock-in allele (*TrkA*$^{+/FLAG}$) is designed to express a diphtheria toxin signal peptide fused N-terminal FLAG-tagged TrkA from a TrkA gene locus (CS, Francis S. Lee and DDG, unpublished). *Ret*$^{+/f}$ mice were described elsewhere (Luo et al., 2007), and were crossed with mice expressing Cre recombinase in the germ cell lineage. The morning after coitus was defined as E0.5.

Antibodies

A rabbit polyclonal antiserum was raised against the GST-fusion protein of an intracellular region of mouse Linx (GST-Linx-C) and affinity-purified. Other antibodies were listed in the Supplemental Procedures.

In Situ Hybridization, Immunocytochemistry, and Immunohistochemistry

Double-fluorescent *in situ* hybridization was performed as previously described (Luo et al., 2007). A detailed description of probes used in this study is available in the Supplemental Data. Immunocytochemistry and immunohistochemistry were performed using standard procedures. Whole-mount immunostaining was performed as described (Huber et al., 2005) and the pictures were taken using a confocal imaging system (LSM 5 Pascal; Carl Zeiss Inc.).

Statistical Analysis

Statistical differences for mean values between two groups and among multiple groups were analyzed using Student's *t* test and Tukey's multiple comparison test, respectively. The criterion for statistical significance was set at $P < 0.05$. All values are reported as the mean ± SEM. A description of the statistical assessment of LIG family gene clusters is available in the Supplemental Data.

Miscellaneous Procedures

The following procedures are available in the Supplemental Section: microarray analysis, generation of DNA constructs, generation of *Linx*$^{+/tEGFP}$ mice, immunoprecipitation procedures, generation of primary neural cultures and qRT-PCR. The extension of nerves and axons was measured using NeuronJ (Meijering et al., 2004).

Supplementary Material

Refer to Web version on PubMed Central for supplementary material.

Acknowledgments

We thank Dr. Frank Rice and members of the Ginty laboratory for helpful discussions and comments on this manuscript. We thank Christopher Deppmann, Nikhil Sharma, Wenqin Luo, Joseph Savitt, Qingguang Jiang, Anthony Harrington and Michael Rutlin for reagents, technical support, and valuable comments; Narendrakumar Ramanan for help with targeting vector design; Dorothy Reimert for ES cell work; Charles Hawkins and the Johns Hopkins Transgenic Facility for blastocyst injections; Francisco Martínez-Murillo, Chunfa Jie and the Johns Hopkins Microarray Core Facility for microarray analysis. This work was supported by National Institutes of Health grants NS34814 (D.D.G.) and NS47348 (M.B). D.D.G. is an investigator of the Howard Hughes Medical Institute.

References

Airaksinen MS, Koltzenburg M, Lewin GR, Masu Y, Helbig C, Wolf E, Brem G, Toyka KV, Thoenen H, Meyer M. Specific subtypes of cutaneous mechanoreceptors require neurotrophin-3 following peripheral target innervation. Neuron 1996;16:287–295. [PubMed: 8789944]

Airaksinen MS, Saarma M. The GDNF family: signalling, biological functions and therapeutic value. Nat Rev Neurosci 2002;3:383–394. [PubMed: 11988777]

Akopian AN, Sivilotti L, Wood JN. A tetrodotoxin-resistant voltage-gated sodium channel expressed by sensory neurons. Nature 1996;379:257–262. [PubMed: 8538791]

Baloh RH, Enomoto H, Johnson EM Jr, Milbrandt J. The GDNF family ligands and receptors - implications for neural development. Curr Opin Neurobiol 2000;10:103–110. [PubMed: 10679429]

Bennett DL, Michael GJ, Ramachandran N, Munson JB, Averill S, Yan Q, McMahon SB, Priestley JV. A distinct subgroup of small DRG cells express GDNF receptor components and GDNF is protective for these neurons after nerve injury. J Neurosci 1998;18:3059–3072. [PubMed: 9526023]

Chen CL, Broom DC, Liu Y, de Nooij JC, Li Z, Cen C, Samad OA, Jessell TM, Woolf CJ, Ma Q. Runx1 determines nociceptive sensory neuron phenotype and is required for thermal and neuropathic pain. Neuron 2006;49:365–377. [PubMed: 16446141]

Crowley C, Spencer SD, Nishimura MC, Chen KS, Pitts-Meek S, Armanini MP, Ling LH, McMahon SB, Shelton DL, Levinson AD, et al. Mice lacking nerve growth factor display perinatal loss of sensory and sympathetic neurons yet develop basal forebrain cholinergic neurons. Cell 1994;76:1001–1011. [PubMed: 8137419]

Ernfors P, Lee KF, Kucera J, Jaenisch R. Lack of neurotrophin-3 leads to deficiencies in the peripheral nervous system and loss of limb proprioceptive afferents. Cell 1994;77:503–512. [PubMed: 7514502]

Fu QL, Hu B, Wu W, Pepinsky RB, Mi S, So KF. Blocking LINGO-1 function promotes retinal ganglion cell survival following ocular hypertension and optic nerve transection. Invest Ophthalmol Vis Sci 2008;49:975–985. [PubMed: 18326721]

Gallarda BW, Bonanomi D, Muller D, Brown A, Alaynick WA, Andrews SE, Lemke G, Pfaff SL, Marquardt T. Segregation of axial motor and sensory pathways via heterotypic trans-axonal signaling. Science 2008;320:233–236. [PubMed: 18403711]

Garces A, Haase G, Airaksinen MS, Livet J, Filippi P, deLapeyriere O. GFRalpha 1 is required for development of distinct subpopulations of motoneuron. J Neurosci 2000;20:4992–5000. [PubMed: 10864957]

Gejima R, Okafuji T, Tanaka H. The LRR and Ig domain-containing membrane protein SST273 is expressed on motoneurons. Gene Expr Patterns 2006;6:235–240. [PubMed: 16378755]

Gould TW, Yonemura S, Oppenheim RW, Ohmori S, Enomoto H. The neurotrophic effects of glial cell line-derived neurotrophic factor on spinal motoneurons are restricted to fusimotor subtypes. J Neurosci 2008;28:2131–2146. [PubMed: 18305247]

Gur G, Rubin C, Katz M, Amit I, Citri A, Nilsson J, Amariglio N, Henriksson R, Rechavi G, Hedman H, et al. LRIG1 restricts growth factor signaling by enhancing receptor ubiquitylation and degradation. EMBO J 2004;23:3270–3281. [PubMed: 15282549]

Hedman H, Henriksson R. LRIG inhibitors of growth factor signalling -double-edged swords in human cancer? Eur J Cancer 2007;43:676–682. [PubMed: 17239582]

Helmbacher F, Schneider-Maunoury S, Topilko P, Tiret L, Charnay P. Targeting of the EphA4 tyrosine kinase receptor affects dorsal/ventral pathfinding of limb motor axons. Development 2000;127:3313–3324. [PubMed: 10887087]

Higgins DG, Bleasby AJ, Fuchs R. CLUSTAL V: improved software for multiple sequence alignment. Comput Appl Biosci 1992;8:189–191. [PubMed: 1591615]

Huang EJ, Reichardt LF. Neurotrophins: roles in neuronal development and function. Annu Rev Neurosci 2001;24:677–736. [PubMed: 11520916]

Huber AB, Kania A, Tran TS, Gu C, De Marco Garcia N, Lieberam I, Johnson D, Jessell TM, Ginty DD, Kolodkin AL. Distinct roles for secreted semaphorin signaling in spinal motor axon guidance. Neuron 2005;48:949–964. [PubMed: 16364899]

Inoue H, Lin L, Lee X, Shao Z, Mendes S, Snodgrass-Belt P, Sweigard H, Engber T, Pepinsky B, Yang L, et al. Inhibition of the leucine-rich repeat protein LINGO-1 enhances survival, structure, and

function of dopaminergic neurons in Parkinson's disease models. Proc Natl Acad Sci U S A 2007;104:14430–14435. [PubMed: 17726113]

Kim S, Burette A, Chung HS, Kwon SK, Woo J, Lee HW, Kim K, Kim H, Weinberg RJ, Kim E. NGL family PSD-95-interacting adhesion molecules regulate excitatory synapse formation. Nat Neurosci 2006;9:1294–1301. [PubMed: 16980967]

Knudson CM, Tung KS, Tourtellotte WG, Brown GA, Korsmeyer SJ. Bax-deficient mice with lymphoid hyperplasia and male germ cell death. Science 1995;270:96–99. [PubMed: 7569956]

Kramer ER, Knott L, Su F, Dessaud E, Krull CE, Helmbacher F, Klein R. Cooperation between GDNF/Ret and ephrinA/EphA4 signals for motor-axon pathway selection in the limb. Neuron 2006a;50:35–47. [PubMed: 16600854]

Kramer I, Sigrist M, de Nooij JC, Taniuchi I, Jessell TM, Arber S. A role for Runx transcription factor signaling in dorsal root ganglion sensory neuron diversification. Neuron 2006b;49:379–393. [PubMed: 16446142]

Kuja-Panula J, Kiiltomaki M, Yamashiro T, Rouhiainen A, Rauvala H. AMIGO, a transmembrane protein implicated in axon tract development, defines a novel protein family with leucine-rich repeats. J Cell Biol 2003;160:963–973. [PubMed: 12629050]

Laederich MB, Funes-Duran M, Yen L, Ingalla E, Wu X, Carraway KL 3rd, Sweeney C. The leucine-rich repeat protein LRIG1 is a negative regulator of ErbB family receptor tyrosine kinases. J Biol Chem 2004;279:47050–47056. [PubMed: 15345710]

Ledda F, Bieraugel O, Fard SS, Vilar M, Paratcha G. Lrig1 is an endogenous inhibitor of Ret receptor tyrosine kinase activation, downstream signaling, and biological responses to GDNF. J Neurosci 2008;28:39–49. [PubMed: 18171921]

Lentz SI, Knudson CM, Korsmeyer SJ, Snider WD. Neurotrophins support the development of diverse sensory axon morphologies. J Neurosci 1999;19:1038–1048. [PubMed: 9920667]

Lin JC, Ho WH, Gurney A, Rosenthal A. The netrin-G1 ligand NGL-1 promotes the outgrowth of thalamocortical axons. Nat Neurosci 2003;6:1270–1276. [PubMed: 14595443]

Lin JH, Saito T, Anderson DJ, Lance-Jones C, Jessell TM, Arber S. Functionally related motor neuron pool and muscle sensory afferent subtypes defined by coordinate ETS gene expression. Cell 1998;95:393–407. [PubMed: 9814709]

Luo W, Wickramasinghe SR, Savitt JM, Griffin JW, Dawson TM, Ginty DD. A hierarchical NGF signaling cascade controls Ret-dependent and Ret-independent events during development of nonpeptidergic DRG neurons. Neuron 2007;54:739–754. [PubMed: 17553423]

MacLaren CM, Evans TA, Alvarado D, Duffy JB. Comparative analysis of the Kekkon molecules, related members of the LIG superfamily. Dev Genes Evol 2004;214:360–366. [PubMed: 15179511]

Markus A, Patel TD, Snider WD. Neurotrophic factors and axonal growth. Curr Opin Neurobiol 2002;12:523–531. [PubMed: 12367631]

Marmigere F, Montelius A, Wegner M, Groner Y, Reichardt LF, Ernfors P. The Runx1/AML1 transcription factor selectively regulates development and survival of TrkA nociceptive sensory neurons. Nat Neurosci 2006;9:180–187. [PubMed: 16429136]

Meijering E, Jacob M, Sarria JC, Steiner P, Hirling H, Unser M. Design and validation of a tool for neurite tracing and analysis in fluorescence microscopy images. Cytometry A 2004;58:167–176. [PubMed: 15057970]

Mi S, Lee X, Shao Z, Thill G, Ji B, Relton J, Levesque M, Allaire N, Perrin S, Sands B, et al. LINGO-1 is a component of the Nogo-66 receptor/p75 signaling complex. Nat Neurosci 2004;7:221–228. [PubMed: 14966521]

Moqrich A, Earley TJ, Watson J, Andahazy M, Backus C, Martin-Zanca D, Wright DE, Reichardt LF, Patapoutian A. Expressing TrkC from the TrkA locus causes a subset of dorsal root ganglia neurons to switch fate. Nat Neurosci 2004;7:812–818. [PubMed: 15247919]

Mu X, Silos-Santiago I, Carroll SL, Snider WD. Neurotrophin receptor genes are expressed in distinct patterns in developing dorsal root ganglia. J Neurosci 1993;13:4029–4041. [PubMed: 8366358]

Nagasawa A, Kubota R, Imamura Y, Nagamine K, Wang Y, Asakawa S, Kudoh J, Minoshima S, Mashima Y, Oguchi Y, et al. Cloning of the cDNA for a new member of the immunoglobulin superfamily (ISLR) containing leucine-rich repeat (LRR). Genomics 1997;44:273–279. [PubMed: 9325048]

Ono T, Sekino-Suzuki N, Kikkawa Y, Yonekawa H, Kawashima S. Alivin 1, a novel neuronal activity-dependent gene, inhibits apoptosis and promotes survival of cerebellar granule neurons. J Neurosci 2003;23:5887–5896. [PubMed: 12843293]

Paratcha G, Ledda F. GDNF and GFRalpha: a versatile molecular complex for developing neurons. Trends Neurosci 2008;31:384–391. [PubMed: 18597864]

Patel TD, Jackman A, Rice FL, Kucera J, Snider WD. Development of sensory neurons in the absence of NGF/TrkA signaling in vivo. Neuron 2000;25:345–357. [PubMed: 10719890]

Patel TD, Kramer I, Kucera J, Niederkofler V, Jessell TM, Arber S, Snider WD. Peripheral NT3 signaling is required for ETS protein expression and central patterning of proprioceptive sensory afferents. Neuron 2003;38:403–416. [PubMed: 12741988]

Povlsen B, Stankovic N, Danielsson P, Hildebrand C. Fiber composition of the lateral plantar and superficial peroneal nerves in the rat foot. Anat Embryol (Berl) 1994;189:393–399. [PubMed: 8092492]

Segal RA. Selectivity in neurotrophin signaling: theme and variations. Annu Rev Neurosci 2003;26:299–330. [PubMed: 12598680]

Shattuck DL, Miller JK, Laederich M, Funes M, Petersen H, Carraway KL 3rd, Sweeney C. LRIG1 is a novel negative regulator of the Met receptor and opposes Met and Her2 synergy. Mol Cell Biol 2007;27:1934–1946. [PubMed: 17178829]

Smeyne RJ, Klein R, Schnapp A, Long LK, Bryant S, Lewin A, Lira SA, Barbacid M. Severe sensory and sympathetic neuropathies in mice carrying a disrupted Trk/NGF receptor gene. Nature 1994;368:246–249. [PubMed: 8145823]

Tessarollo L, Vogel KS, Palko ME, Reid SW, Parada LF. Targeted mutation in the neurotrophin-3 gene results in loss of muscle sensory neurons. Proc Natl Acad Sci U S A 1994;91:11844–11848. [PubMed: 7991545]

Tran TS, Kolodkin AL, Bharadwaj R. Semaphorin regulation of cellular morphology. Annu Rev Cell Dev Biol 2007;23:263–292. [PubMed: 17539753]

White FA, Keller-Peck CR, Knudson CM, Korsmeyer SJ, Snider WD. Widespread elimination of naturally occurring neuronal death in Bax-deficient mice. J Neurosci 1998;18:1428–1439. [PubMed: 9454852]

Wichterle H, Lieberam I, Porter JA, Jessell TM. Directed differentiation of embryonic stem cells into motor neurons. Cell 2002;110:385–397. [PubMed: 12176325]

Wickramasinghe SR, Alvania RS, Ramanan N, Wood JN, Mandai K, Ginty DD. Serum response factor mediates NGF-dependent target innervation by embryonic DRG sensory neurons. Neuron 2008;58:532–545. [PubMed: 18498735]

Wu M, Huang C, Gan K, Huang H, Chen Q, Ouyang J, Tang Y, Li X, Yang Y, Zhou H, et al. LRRC4, a putative tumor suppressor gene, requires a functional leucine-rich repeat cassette domain to inhibit proliferation of glioma cells in vitro by modulating the extracellular signal-regulated kinase/protein kinase B/nuclear factor-kappaB pathway. Mol Biol Cell 2006;17:3534–3542. [PubMed: 16723503]

Zhao H, Tanegashima K, Ro H, Dawid IB. Lrig3 regulates neural crest formation in Xenopus by modulating Fgf and Wnt signaling pathways. Development 2008;135:1283–1293. [PubMed: 18287203]

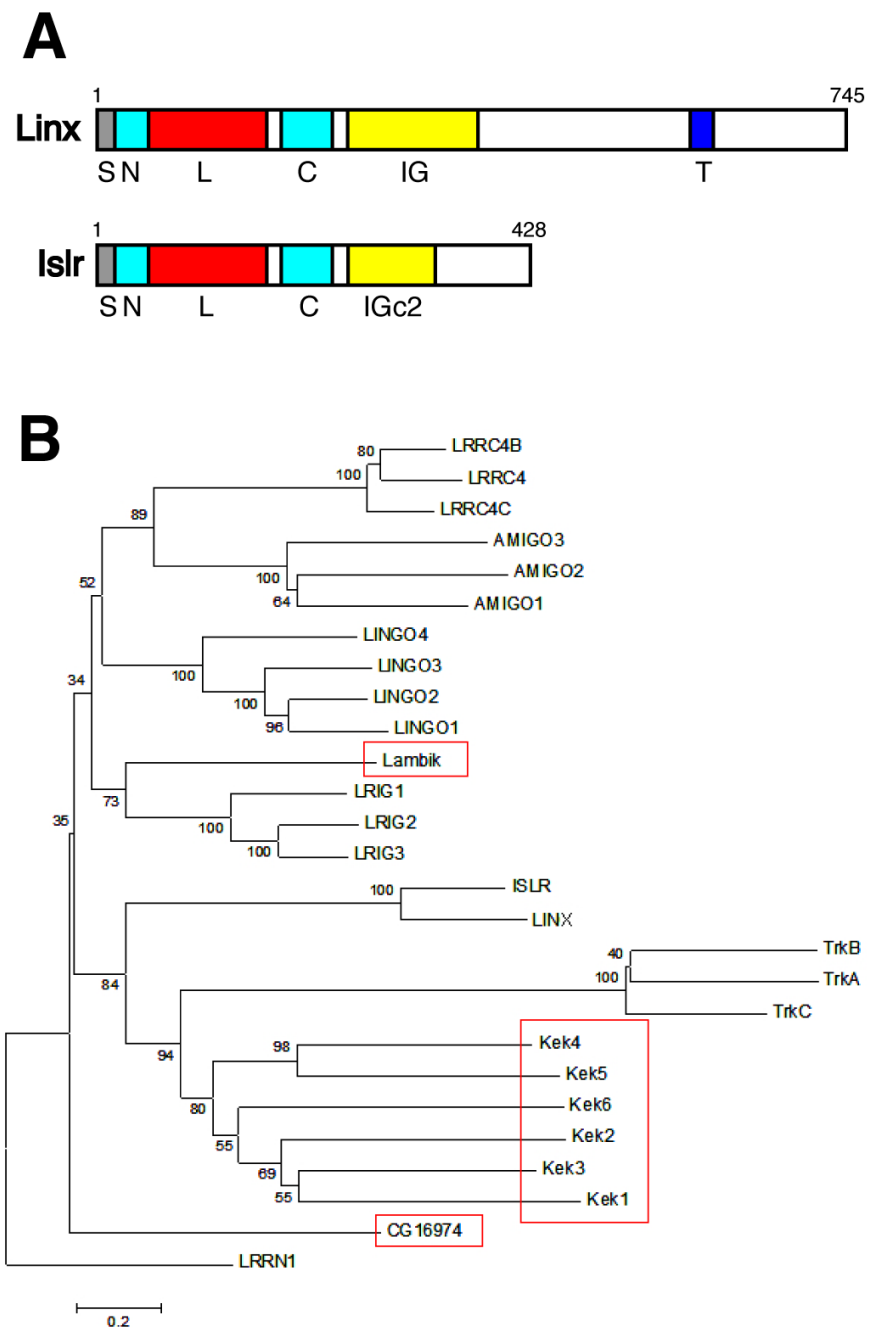

Figure 1. Linx Is a LIG Family Member

(A) Domain organizations of Linx and Islr. S: signal peptide, N: leucine rich repeat N-terminal domain, L: leucine-rich repeat domains, C: leucine rich repeat C-terminal domain, IG: immunoglobulin domain, IGc2: immunoglobulin c2-type domain, T: transmembrane domain. (B) Molecular phylogenetic analysis of human and Drosophila LIG family members. The extracellular protein sequences were aligned using the ClustalV software (Higgins et al., 1992). The branch lengths are proportional to the number of amino acid changes. Drosophila LIGs are encircled with red boxes. Note that a rooted tree was generated designating human LRRN1, a more distantly related gene composed of LRRNT, LRR, LRRCT, IGc2 and fibronectin type 3 domains, as an out-group.

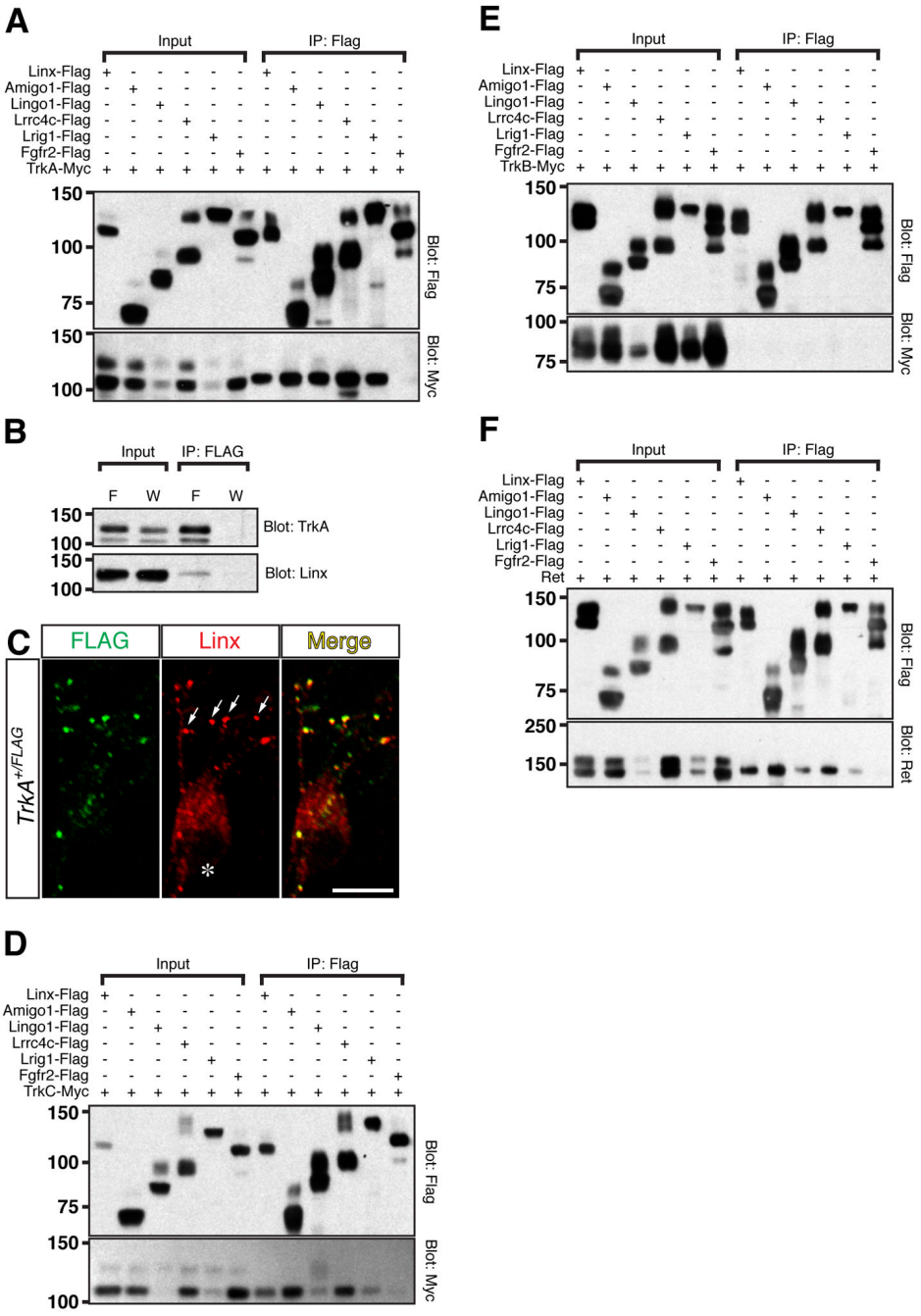

Figure 2. Binding of LIG Family Proteins to Trk and Ret Receptor Tyrosine Kinases

(A, D, E, F) Various combinations of recombinant proteins were expressed in 293T cells and subjected to immunoprecipitation experiments using a FLAG antibody. The precipitates were then examined by Western blot analysis to examine interactions with TrkA (A), TrkC (D), TrkB (E) and Ret (F). Protein molecular weight standards (kDa) are shown on the left side of blots.

(B) Physical interaction of endogenous Linx and TrkA. Cultured DRG neurons obtained from E13.5 *FLAG epitope tagged-TrkA* knock-in ($TrkA^{FLAG/FLAG}$) and wild-type mice were subjected to immunoprecipitation using a FLAG antibody. The precipitates were examined by Western blot analysis to examine interaction. F: $TrkA^{FLAG/FLAG}$, W: wild-type.

(C) Confocal microscopic images of cultured DRG neurons obtained from E13.5 *FLAG epitope tagged-TrkA* knock-in mice. Endogenous FLAG-TrkA and Linx were detected with FLAG (green) and Linx antibodies (red). Arrows: examples of vesicle-like structures in axons, asterisk: a nucleus of a DRG neuron, bar: 10 μm.

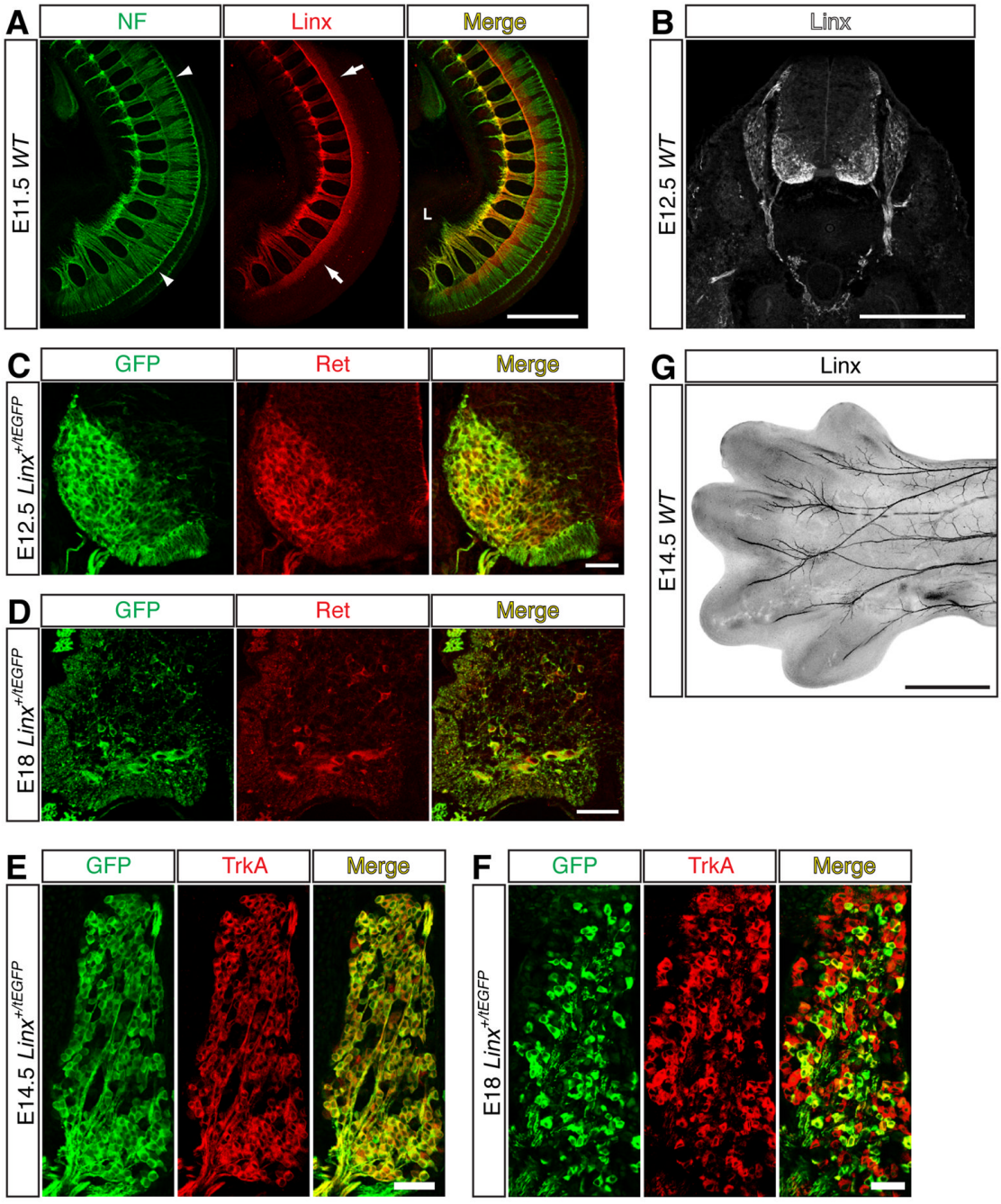

Figure 3. Expression of Linx in Motor and Sensory Neurons

(A) A Z-Stack confocal image for the lateral half of an E11.5 wild-type embryo stained by whole-mount anti-Neurofilament-M (green) and anti-Linx (red) immunostaining. Arrows: ventral spinal cord, arrowheads: dorsal root entry zone, L: lumbar plexus, bar: 0.5 mm.

(B) A transverse section of lumbar spinal cord and DRGs of an E12.5 wild-type embryo stained with a Linx antibody. Bar: 0.5 mm.

(C and D) Horizontal sections of lumbar spinal cords of *Linx*$^{+/tEGFP}$ embryos stained with GFP (green) and Ret (red) antibodies at E12.5 (C) and E18 (D). Bars: 50 μm.

(E and F) Horizontal sections of lumbar DRGs of *Linx*$^{+/tEGFP}$ embryos stained with GFP (green) and TrkA (red) antibodies at E14.5 (E) and E18 (F). Bars: 50 μm.

(G) A Z-Stack confocal image of a dorsal view of an E14.5 wild-type left hindlimb visualized by whole-mount anti-Linx immunostaining. Bar: 0.5 mm.

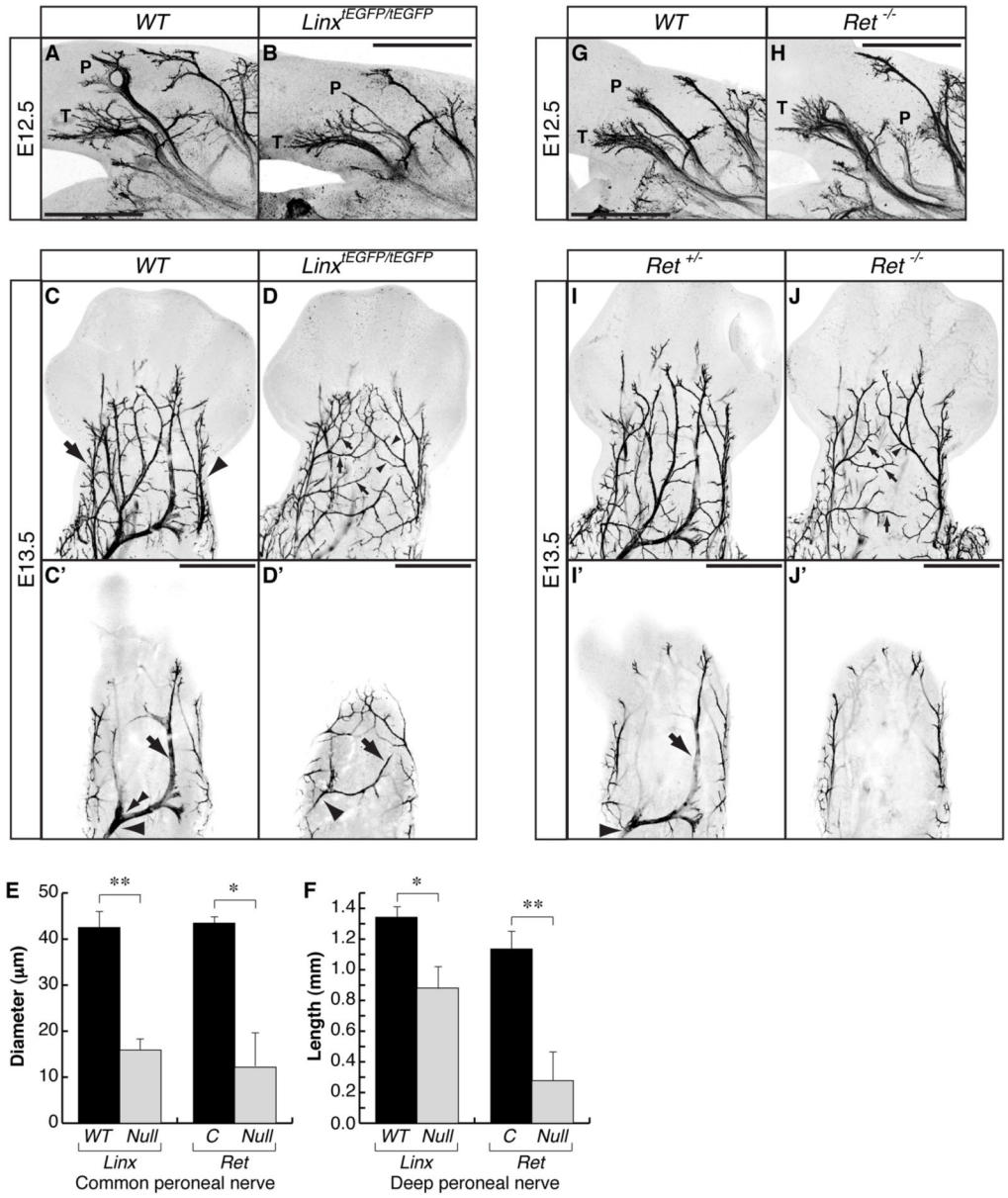

Figure 4. *Linx* Mutant Mice Partially Phenocopy *Ret* Mutant Mice, and Linx Functions in the GDNF-Ret Signaling Pathway

(A–D) Whole-mount anti-Peripherin immunostaining of left hindlimbs of *Linx*$^{tEGFP/tEGFP}$ (B, D and D′) and wild-type (A, C and C′) embryos at E12.5 (A and B) and E13.5 (C, C′, D and D′). WT: wild-type, bars: 0.5 mm.

(A and B) Z-Stack confocal images of representative posterior views of left hindlimbs taken from 4 *Linx*$^{tEGFP/tEGFP}$ and wild-type embryos. Note that the dramatic decrease in length and size of peroneal nerve in *Linx*$^{tEGFP/tEGFP}$ embryos. P: peroneal nerve, T: tibial nerve.

(C, C′, D and D′) Z-Stack confocal images of dorsal views of left hindlimbs (C and D) and their raw images depicting common and deep peroneal nerves (C′ and D′). Arrow: sural nerve, arrowhead: saphenous nerve (C). Small arrows: aberrant branches from sural nerve, small arrowheads: aberrant branches from saphenous nerve (D). Arrows: deep peroneal nerves, arrowheads: common peroneal nerves (C′ and D′). Double arrowhead: a point where a common peroneal nerve divides into superficial and deep peroneal nerves (C′)

(E) Average diameter of the common peroneal nerve in *Linx*$^{tEGFP/tEGFP}$ (n=9) compared to wild-type control embryos (n=8) (left), as well as that of *Ret*$^{-/-}$ (n=7) compared to control embryos (n=6) (right). The 6 control embryos for *Ret*$^{-/-}$ in E and F are composed of 2 wild-type and 4 *Ret*$^{+/-}$. C: control. * and ** indicate $p<0.005$ and $p<5\times10^{-5}$, respectively.
(F) Average length of the deep peroneal nerve in *Linx*$^{tEGFP/tEGFP}$ (n=9) compared to wild-type control embryos (n=9) (left), as well as that of *Ret*$^{-/-}$ (n=7) compared to control embryos (n=6) (right). The length of the deep peroneal nerve was measured from a branching point (double arrowhead shown in C′) to a distal end of the nerve. C: control. * and ** indicate $p<0.01$ and $p<0.005$, respectively.
(G–J) Whole-mount anti-Peripherin immunostaining of left hindlimbs of *Ret*$^{-/-}$ (H, J and J′), wild-type (G) and control *Ret*$^{+/-}$ (I and I′) embryos at E12.5 (G and H) and E13.5 (I, I′, J and J′). Bars: 0.5 mm.
(G and H) Z-Stack confocal images of representative posterior views of left hindlimbs of 3 *Ret*$^{-/-}$ and wild-type embryos. P: peroneal nerve, T: tibial nerve.
(I, I′, J and J′) Z-Stack confocal images of dorsal views of left hindlimbs (I and J) and their raw images depicting common and deep peroneal nerves (I′ and J′). Small arrows: aberrant branches from sural nerve, small arrowhead: aberrant branches from saphenous nerve (J). Arrow: deep peroneal nerve, arrowhead: common peroneal nerve (I′).

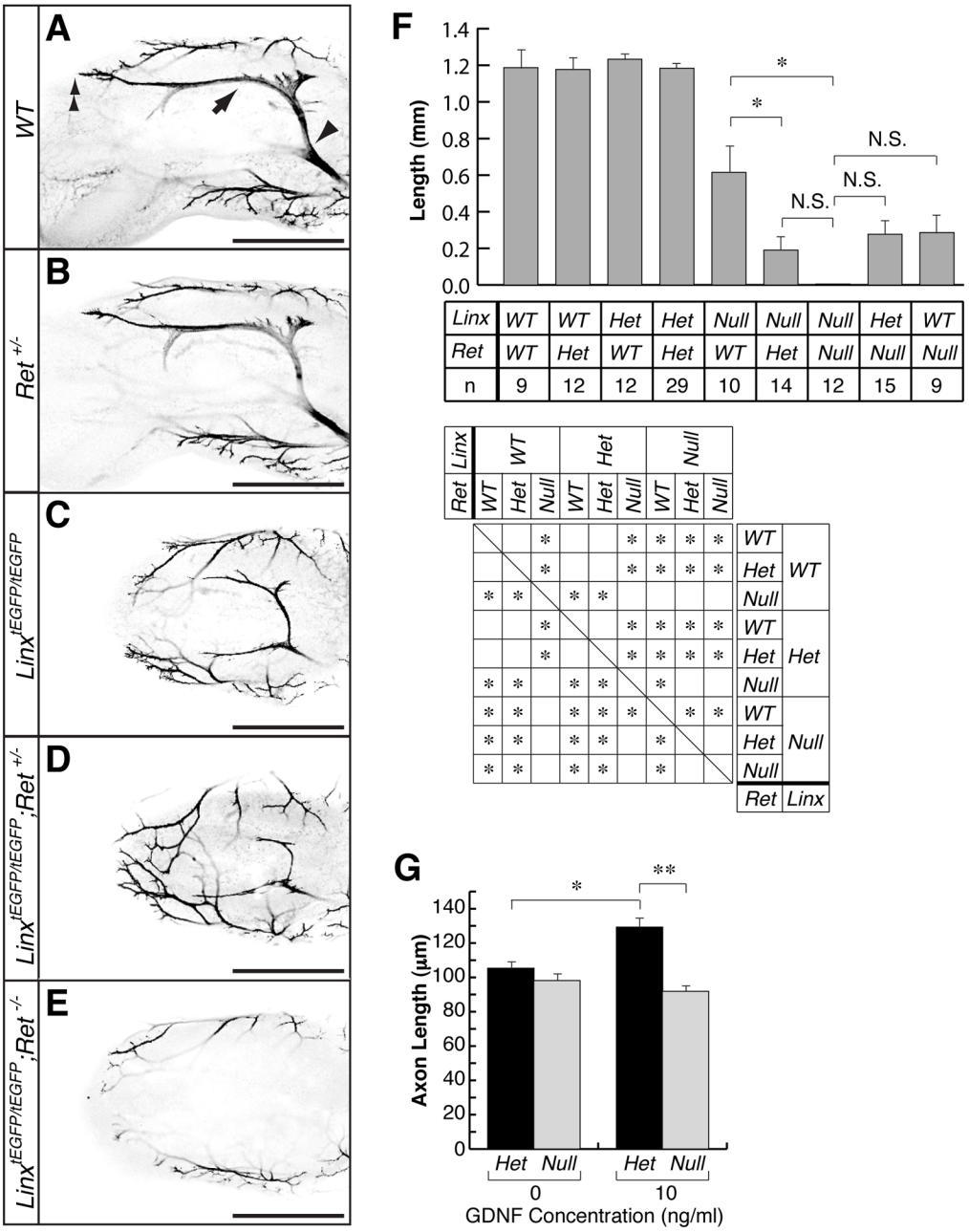

Figure 5. Functional Interaction between *Linx* and *Ret*

(A–E) Confocal images for anti-Peripherin immunostaining of left hindlimbs of wild-type (A), $Ret^{+/-}$ (B), $Linx^{tEGFP/tEGFP}$ (C), $Linx^{tEGFP/tEGFP};Ret^{+/-}$ (D) and $Linx^{tEGFP/tEGFP};Ret^{-/-}$ (E) embryos at E13.5. WT: wild-type, arrow: deep peroneal nerve, arrowhead: the point where the common peroneal nerve divides into superficial and deep peroneal nerves, double arrowhead: distal end of the deep peroneal nerve branch to the 2nd an 3rd digits, bars: 0.5 mm. Note that peroneal nerves are completely absent in $Linx^{tEGFP/tEGFP};Ret^{-/-}$ (E).

(F) Length of the deep peroneal nerve in various mutants. The length of the deep peroneal nerve was measured from the dividing point (arrowhead in A) to the end of the digital branch to the 2nd and 3rd digits (double arrowhead in A). In the case of absence of the peroneal nerves, the value is considered as zero. Statistical analysis was performed using multiple comparison

test. The table shows significance of the difference of mean values. * indicates $p<0.05$. N.S.: not significant, het: heterozygous, n: number of embryos analyzed for each group.

(G) Linx is required for GDNF-dependent motor axon extension. Average axon length of cultured lumbar motor neurons obtained from E13.5 $Linx^{tEGFP/tEGFP}$ and $Linx^{+/tEGFP}$ control embryos. Lumbar motor neurons were cultured in growth media containing CNTF (10 ng/ml) and either the presence or absence of GDNF (10 ng/ml) for 24hr and axonal lengths (n=174 to 200 cells for each condition) were measured of GFP^+ and $Islet1^+$ neurons. * and ** indicate $p<0.0005$ and $p<1X10^{-10}$, respectively.

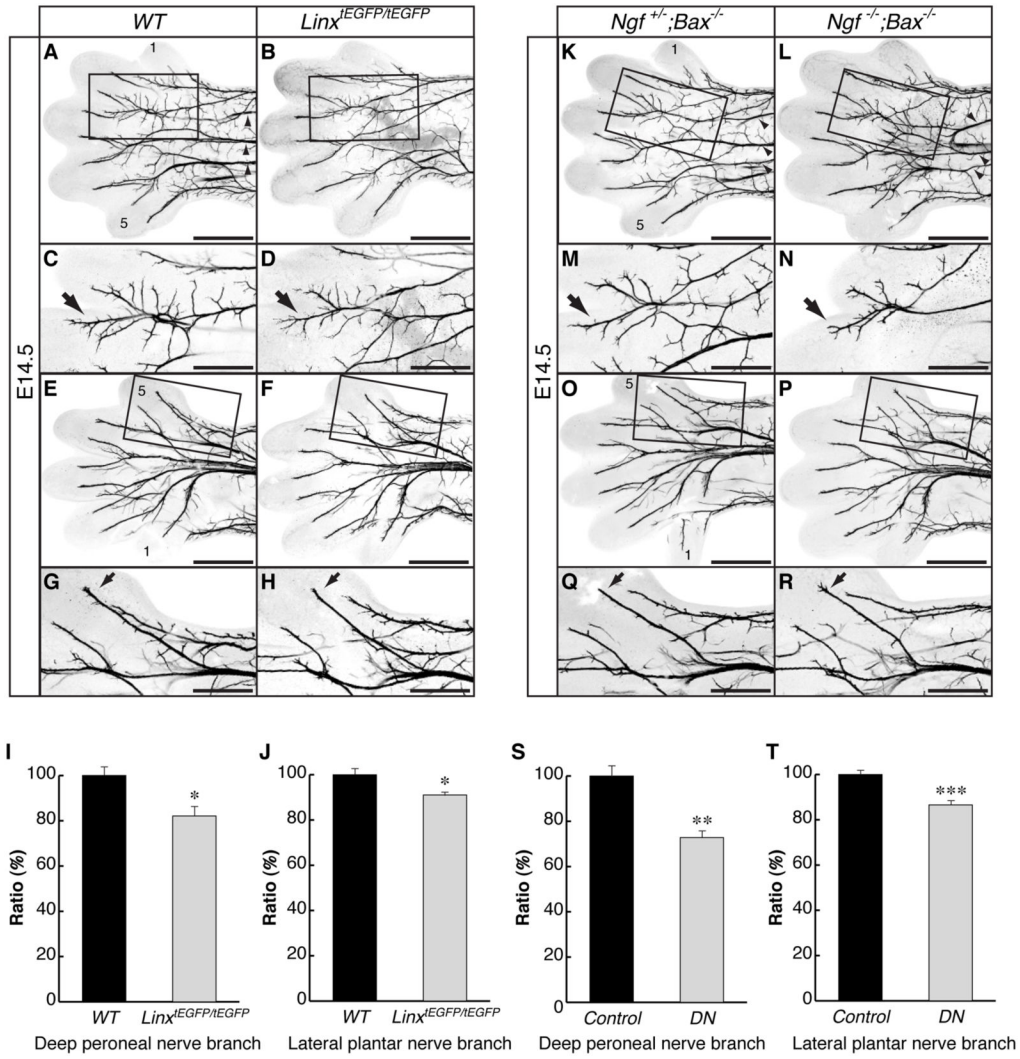

Figure 6. *Linx* Mutant Mice Partially Phenocopy *Ngf* Mutant Mice in Nerve Extension Defects

(A–H) Whole-mount anti-Peripherin immunostaining of left hindlimbs of *Linx*$^{tEGFP/tEGFP}$ (B, D, F and H) and wild-type (A, C, E and G) embryos at E14.5. WT: wild-type, 1 and 5: the 1st and 5th digit. Bars: 0.5 mm in A, B, E and F; 0.25 mm in C, D, G and H.

(A and B) Z-Stack confocal images of a dorsal view of the left hindlimb. Boxes: magnifications are shown in C and D, arrowheads: peroneal nerve branches.

(C and D) High-magnification Z-stack confocal images showing digital branches of the deep peroneal nerve in the 2nd and 3rd digits. Arrows: digital branches to the 3rd digits.

(E and F) Z-Stack confocal images of a plantar view of the left hindlimb. Boxes: magnifications are shown in G and H.

(G and H) High-magnification Z-stack confocal images showing a lateral digital branch of the lateral plantar nerve in the 5th digit. Arrows: lateral digital branches of the lateral plantar nerve in the 5th digit.

(I) Average ratio of the length of a digital branch of the deep peroneal nerve in the 3rd digit of *Linx*$^{tEGFP/tEGFP}$ (n=11) compared to wild-type (n=13) embryos. * indicates p<0.01.

(J) Average ratio of the length of a lateral digital branch of the lateral plantar nerve in the 5th digit of *Linx*$^{tEGFP/tEGFP}$ (n=9) compared to wild-type (n=10) embryos. * indicates p<0.01.

(K–R) Whole-mount anti-Peripherin immunostaining of left hindlimbs of *Ngf*$^{-/-}$;*Bax*$^{-/-}$ (L, N, P and R) and *Ngf*$^{+/-}$;*Bax*$^{-/-}$ control (K, M, O and Q) embryos at E14.5. 1 and 5: the 1st and 5th digit. Bars: 0.5 mm in K, L, O and P; 0.25 mm in M, N, Q and R.

(K and L) Z-Stack confocal images of a dorsal view of the left hindlimb. Boxes: magnifications are shown in M and N, arrowheads: peroneal nerve branches. Note that peroneal nerve branches are formed in the *Ngf*$^{-/-}$;*Bax*$^{-/-}$ embryo as the control embryo.

(M and N) High-magnification Z-stack confocal images showing digital branches of the deep peroneal nerve in the 2nd and 3rd digits. Arrows: digital branches to the 3rd digit.

(O and P) Z-Stack confocal images of a plantar view of the left hindlimb. Boxes: magnifications are shown in Q and R.

(Q and R) High-magnification Z-stack confocal images showing a lateral digital branch of the lateral plantar nerve in the 5th digit. Arrows: lateral digital branches of the lateral plantar nerve in the 5th digit.

(S) Average ratio of the length of a digital branch of the deep peroneal nerve in the 3rd digit of *Ngf*$^{-/-}$;*Bax*$^{-/-}$ (n=7) compared to *control* (n=7) embryos. *Control* embryos in S and T are composed of 2 *Bax*$^{-/-}$, 1 *Bax*$^{+/-}$, 2 *Ngf*$^{+/-}$;*Bax*$^{-/-}$ and 2 wild-type. DN: *Ngf* $^{-/-}$;*Bax*$^{-/-}$. ** indicates $p<0.005$.

(T) Average ratio of the length of a lateral digital branch of the lateral plantar nerve in the 5th digit of *Ngf*$^{-/-}$;*Bax*$^{-/-}$ (n=7) compared to *control* (n=7) embryos. DN: *Ngf*$^{-/-}$;*Bax*$^{-/-}$. *** indicates $p<0.0005$.

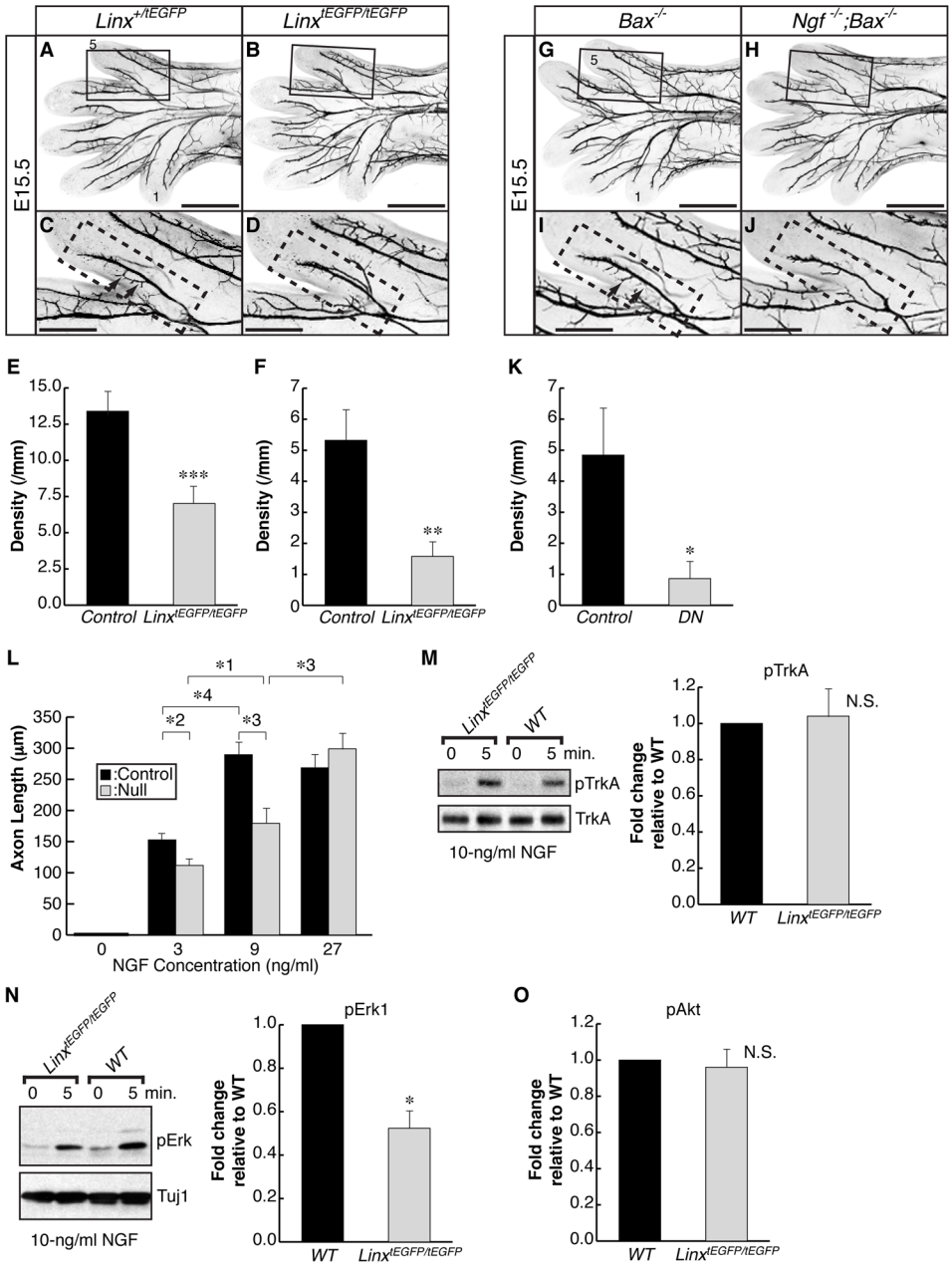

Figure 7. *Linx* Mutant Mice Partially Phenocopy *Ngf* Mutant Mice in Nerve Branching Defects, and Linx Functions in the NGF Signaling Pathway

(A–D) Whole-mount anti-Peripherin immunostaining of left hindlimbs of *Linx*$^{tEGFP/tEGFP}$ (B and D) and *Linx*$^{+/tEGFP}$ control (A and C) embryos at E15.5. Bars: 0.625 mm in A and B; 0.25 mm in C and D.

(A and B) Z-Stack confocal images of a plantar view of the left hindlimb. Boxes: magnifications are shown in C and D, 1 and 5: the 1st and 5th digit.

(C and D) High-magnification Z-stack confocal images showing a medial digital branch of the lateral plantar nerve in the 5th digit. Dotted rectangles: medial digital branches of the lateral plantar nerve in the 5th digit, arrows: representative branches with higher-ordered branches.

(E and F) Density of branches (E) and density of branches with higher-ordered branches (F) in the medial digital branch of the lateral plantar nerve of the 5th digit in *Linx*$^{tEGFP/tEGFP}$ (n=12)

compared to *control* (*Linx*$^{+/tEGFP}$: n=6; wild-type: n=3) embryos. ** and *** indicates p<0.005 and p<0.001, respectively.

(G–J) Whole-mount anti-Peripherin immunostaining of left hindlimbs of *Ngf*$^{-/-}$;*Bax*$^{-/-}$ (H and J) and *Bax*$^{-/-}$ control (G and I) embryos at E15.5. Bars: 0.625 mm in G and H; 0.25 mm in I and J.

(G and H) Z-Stack confocal images of a plantar view of the left hindlimb. Boxes: magnifications are shown in I and J, 1 and 5: the 1st and 5th digit.

(I and J) High-magnification Z-stack confocal images showing a medial digital branch of the lateral plantar nerve in the 5th digit. Dotted rectangles: medial digital branches of the lateral plantar nerve in the 5th digit, arrows: representative branches with higher-ordered branches.

(K) Density of branches with higher-ordered branches in the medial digital branch of the lateral plantar nerve in the 5th digit of *Ngf*$^{-/-}$;*Bax*$^{-/-}$ (n=4) compared to *control* (*Bax*$^{-/-}$: n=2; *Bax*$^{+/-}$: n=1; *Ngf*$^{+/-}$;*Bax*$^{+/-}$: n=1) embryos. DN: *Ngf*$^{-/-}$;*Bax*$^{-/-}$. * indicates p<0.05.

(L) Linx is required for maximal sensitivity to NGF in cultured DRG sensory neurons. Average axon length of cultured DRG sensory neurons obtained from E13.5 *Linx*$^{tEGFP/tEGFP}$ and *Linx*$^{+/tEGFP}$ control embryos. DRG sensory neurons were grown in the presence of 0, 3, 9 and 27 ng/ml NGF with a caspase inhibitor, BAF, for 24 hr and axon lengths (n=40 to 47 cells for each condition) were measured for GFP^{+} neurons using Neurofilament-M staining. *1, *2, *3 and *4 indicates p<0.01, p<0.005, p<0.001 and p<5×10^{-7}, respectively.

(M–O) Phosphorylation of TrkA, Erk and Akt in cultured DRG sensory neurons obtained from E13.5 *Linx*$^{tEGFP/tEGFP}$ and wild-type embryos. DRG sensory neurons were stimulated with NGF (10 ng/ml) for 5 min and phosphorylation of TrkA Y490 (M), Erk (N) and Akt (O) were examined by Western blot analysis. Immunoblots were then reprobed with a class III β-Tublin (Tuj1) or TrkA antibody. The bands for phosphorylated proteins from 4 independent experiments were measured by densitometry, and fold changes of the band intensity in *Linx*$^{tEGFP/tEGFP}$ were calculated against that in wild-type after normalizing with the signal intensities of Tuj1 for pErk and pAkt blots or TrkA for a pTrkA blot. WT: wild-type, N.S.: not significant. * indicates p<0.01.

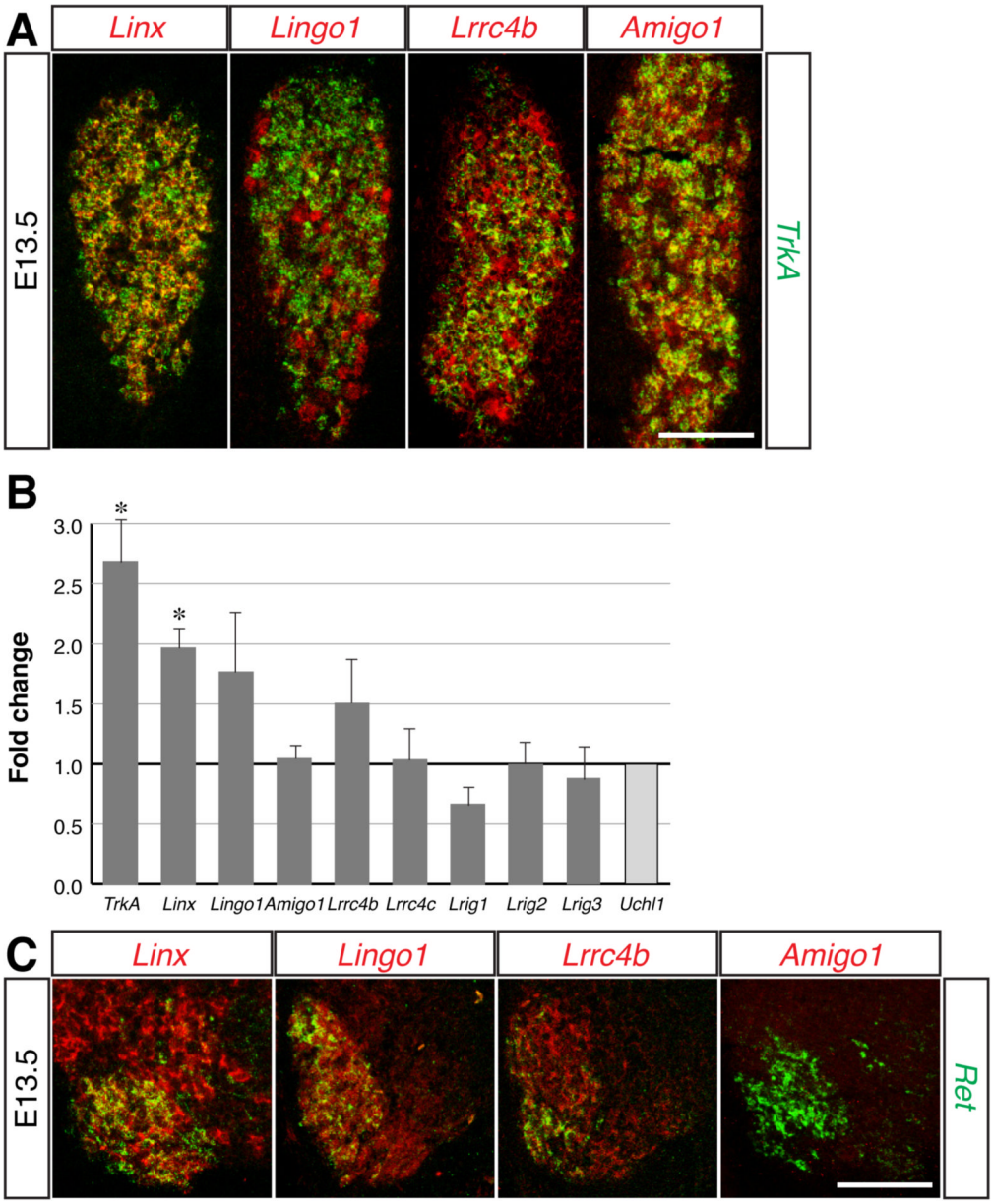

Figure 8. Expression of *LIG* Family Members in the DRG and Ventral Spinal Cord

(A and C) Double-label *in situ* hybridization of *Linx*, *Lingo1*, *Lrrc4b* and *Amigo1* (red) with *TrkA* (A) or *Ret* (C) (green). E13.5 DRG and spinal cord sections were hybridized with indicated cRNA probes. Bars, 100 μm.

(B) NGF-dependent induction of *LIG* family members. The expression of the indicated genes was evaluated by qRT-PCR. Total RNAs were obtained from three independent sets of E13.5 explant DRG cultures grown in the presence or absence of NGF (25 ng/ml). The extent of the gene induction by NGF was evaluated and reported as fold change (>1). * indicates $p<0.05$ using a paired t-test.